THEORETICAL AND APPLIED MECHANICS
Volume 45 (2018) Issue 2, 151–165 DOI: https://doi.org/10.2298/TAM171201010S

EXPERIMENTAL AND NUMERICAL ANALYSIS OF FLOW FIELD AND VENTILATION PERFORMANCE IN A TRAFFIC TUNNEL VENTILATED BY AXIAL FANS

Milan Šekularac and Novica Janković

Abstract. To investigate air flow in longitudinally ventilated traffic tunnels, a scaled model of a typical road-traffic tunnel with an appropriate ventilation system based on axial ducted fans, is designed and built in the Lab. The focus of this paper is the airflow in a bi-directional traffic, two-lane tunnel. At the scale ratio of approx. 1:20, at 20.52 m length it represents ≈ 400 m of a real-scale tunnel. The model consists of two parallel tunnel tubes, where the main tunnel (with a hydraulic diameter of $D_{h1} \approx 0.4$ m) has the geometry of a scaled road traffic-tunnel. The second tunnel ($D_{h2} \approx 0.16$ m) has a smaller size and is circular in cross-section, used only to simulate airflow towards an evacuation tunnel tube. Thus the two tunnels are connected by the evacuation passages, equipped with adjustable escape doors. By a combination of experimental and numerical work, the air flow-field and the performance of the ventilation system are investigated. The velocity field and its turbulence properties exiting the fans were determined experimentally using hot-wire anemometry. These data were further processed to be used in the tunnel flow computations by CFD. The efficiency of momentum transfer (η_i, Kempf factor) of the longitudinal tunnel ventilation is determined. The effect that the imposed boundary conditions and the level of their detail, have within a CFD computation of tunnel airflow, with respect to accuracy, velocity distribution and computed η_i. Finally a traffic-loaded (traffic "jam") case of flow is studied through experiment and CFD. The difficulty in assessing the required thrust of the plant in traffic-jam tunnel conditions is discussed, and the ventilation efficiency is estimated. Based on later results, the two limiting shapes of axial velocity distribution with respect to height above the road, in this type of tunnel and traffic, are estimated. The last result can be used as a realistic boundary condition (as inlet b.c. and/or initial condition) for numerical studies of flow and fire scenarios in such tunnels with the traffic load critical for design.

2010 *Mathematics Subject Classification:* 76-05; 76D99; 76F99.

Key words and phrases: ventilation flows, tunnels, axial ducted fans, turbulence, numerical boundary conditions, CFD.

The paper is presented at the 6$^{\text{th}}$ Serbian Congress in Theoretical and Applied Mechanics (19—21 June 2017), Minisimposia Turbulence. The paper is a part of the collection of papers from the Congress published in the issue 1 of the same volume.

1. Introduction

A review of different design concepts for traffic tunnel ventilation can be found in [**1**]. Recent advances in the field related to the design of more energy efficient ventilation systems can be found in [**2**]. Consider here a longitudinal ventilation system with axial ducted fans, attached to the tunnel ceiling, which can exert a static thrust T, and the effective thrust exerted by these fans to the traffic tunnel's airstream is $T_{\rm ef}$:

$$T = \rho \cdot A_f \cdot w^2, \quad T_{\rm ef} = N \cdot T \cdot \Big(1 - \frac{v_t}{w}\Big) \cdot \eta_i = N \cdot T \cdot k_1 \cdot \eta_i, \tag{1.1}$$

where: w is the mean axial velocity of the fan's jet, v_t the tunnel air-stream mean velocity, A_f is the fan exit's cross sectional area, while the $T_{\rm ef}$ is the effective thrust exerted on the tunnel's air flow by the system equipped with N fans, [**1**, **3**]. Factor k_1 denotes the influence of the mean axial velocity of the tunnel flow which offloads the fan, while η_i factor is usually referred to as installation efficiency, Kempf factor [**1**, **2**], and denotes the efficiency of momentum transfer from the jet fans to the air stream in the tunnel. Factor k_1 is of kinematic character, it can be increased only by increasing the velocity of the jet at the fan's exit, since the tunnel air-stream velocity is predetermined by ventilation design requirements. Some authors split the η_i into two factors: k_2 and k_3. The former should account for the influence of the relative separation between the tunnel ceiling and the fan's axis, while the later should account for the possible downward tilting of the fan's jet axis with respect to the tunnel longitudinal axis, which can increase the η_i. In this paper the distance of the fan axis to the ceiling had a common value of approximately equal to fan diameter and the fan axis was parallel to the tunnel axis. Aside the aforementioned aspects, the overall energy efficiency of the ventilation system is influenced by the hydraulic efficiency of the fan which is in the $\sim$0.40–0.80 range and the motor efficiency $\sim$0.90–0.95. These factors greatly decrease the overall energy efficiency of the system, whereas the space for improvement is mainly related to the increase of the fan hydraulic efficiency, the fan's jet velocity and the momentum transfer efficiency η_i [**2**]. The effective thrust required to push the air-flow in the tunnel can, in principle, be determined by using the following formula [**1**, eq. 3]:

$$\begin{aligned} T = \Big(\zeta_{\rm in} + \xi\frac{L_t}{D_h} + 1\Big) A_t \rho v_{\rm tun}^2/2 + \sum_{\rm veh^+} \zeta_+ A_i \rho (v_v + v_{\rm tun})^2/2 \\ + \sum_{\rm veh^-} \zeta_- A_i \rho (v_v - v_{\rm tun})^2/2, \end{aligned} \tag{1.2}$$

where v_v is the absolute value of vehicle velocity, the ς_+, ς_- denote the hydraulic resistance coefficients of the vehicles in their streamlined and their opposite orientations, respectively (for a bi-directional traffic situation studied here), whereas the dynamic pressure term is computed using the absolute value of the air's relative velocity with respect to the vehicle.

The aforementioned efficiency factor η_i is dependent on the properties of the turbulent flow generated by the fans, in particular the secondary flow components of the exiting jet swirl [**3**–**5**]. However, in the published studies with numerical

simulation of tunnel airflow, the fans are usually represented as momentum sources or jets of a constant axial (mean-flow) velocity w. The w value is predetermined by the available fan's static thrust measurements [**2**, **6**, **7**].

On the other hand, the results of the available experimental studies on fire and smoke movement in the tunnel are based on experiments obtained using scaled laboratory installations where the airflow in the model-tunnel is induced by an external source (fan or pressure tank) through a flow-straightening honeycomb, so the velocity profiles in the tunnel are flat when they approach the fire source [**8**–**12**].

The properties of flow generated at the fan's exit will indirectly influence the smoke movement and control. The fan design, possible fan jet tilting, will affect the axial velocity distribution [**13**]. It is noted [**12**] that a more efficient design will reduce the friction losses on the tunnel ceiling and redistribute the axial velocity by lowering its value near the ceiling, which may promote smoke back-layering. One can expect the changes in velocity distribution to have an effect of vertical stratification of temperature and pollutant fields too. Some recent papers address this topic with respect to fan location and other inputs, in an empty tunnel flow case [**13**]. These effects should be further investigated. For the smoke control problem, an overview of the available literature results for estimating the critical velocity and smoke back-layering length is given in [**14**].

This paper attempts to give a better insight into the details of the flow field and the results accuracy attainable through CFD, with respect to used boundary conditions. An experiment in the Lab tunnel model is used for verification.

2. Experimental results

The sketch of the built experimental installation [**3**] and the CAD model of the utilized axial fans are shown in Figure 1.

The installation consists of two parallel tunnel tubes: the main tunnel (at a scale ratio $\approx 1:20$, shaped as a road-traffic tunnel) with a hydraulic diameter of $D_{h1} \approx 0.40\,\mathrm{m}$) and a secondary tunnel tube circular in cross section ($D_{h2} = 0.16\,\mathrm{m}$), which can simulate airflow from/to an evacuation tunnel tube. Tunnels are connected to the evacuation tunnel by three evacuation passages (EP), and are approx. 100 fan diameters DF apart, equipped with shut-off valves. The characteristic distance L between fan batteries (F1F2, F3F4, F5F6) is approx. $\sim 5\,\mathrm{m}$ or ~ 100 fan diameters, or $12.5\,D_{h1}$. At $L_t = 4L = 20\,520\,\mathrm{mm}$ tunnel length the installation corresponds to approx. 400 m of a real-scale traffic tunnel.

2.1. Experimental results. The utilized fans are model-aircraft vehicle (UAV) propulsion axial fans by Great Planes "Hyperflow" with a 55 mm rotor diameter, the rotor spinning rate in the results reported in this paper was 27 500 RPM. The fan exerts approx. 2.28 N of static thrust and generates a jet with a mean axial exit velocity $w = 34.5\,\mathrm{m/s}$. The detailed results of experimental study on the turbulent flow generated with such fans can be found in [**16**] where a hot-wire anemometry measurement-system with an appropriate signal processing procedure was utilized to determine the flow. The details on hot-wire probe design and the measurement setup can be found in [**17**]. The mean value of axial velocity at fan

exit obtained by static thrust measurements on the test-table and use of eq. (1.1) agree very well with the value obtained by numerical integration of the measured turbulent flow field. A comparison of these results with larger-scale fans reveals that the dimensionless profiles of turbulence kinetic energy, turbulence intensity, and the dimensionless Reynolds stresses, show very similar profiles and maximum values for this fan compared to larger-scale fans (larger by a factor of $\sim$10–20, at approx. correspondingly lower rotor speeds, typically $\sim$ 1500 RPM), **[3]**. The time-averaged axial, radial and tangential components of fan's flow field, given in detail in **[3, 16]** are presented in Figure 2.

The average values of yaw and pitch angles are: 3° and 2.3° respectively. By utilizing the definition for total turbulent fluctuations **[3]**, graphs of time-averaged turbulent intensity Tu and dimensionless turbulent kinetic energy TKE were computed **[3]**, used further in this paper, see Figure 4.

The maximum and mean-value of dimensionless TKE over the flow-exit area are approx. 0.33 % and 0.10 %. The turbulence intensity mean-value is 4.41 % whereas the maxima are at 13.1 %. Fan exit zones are the areas of the highest turbulence intensities in the tunnel.

The hydraulic properties of the installation were measured in the Lab: the effective relative roughness of the tunnel tubes (0.00035), the entry losses coefficient

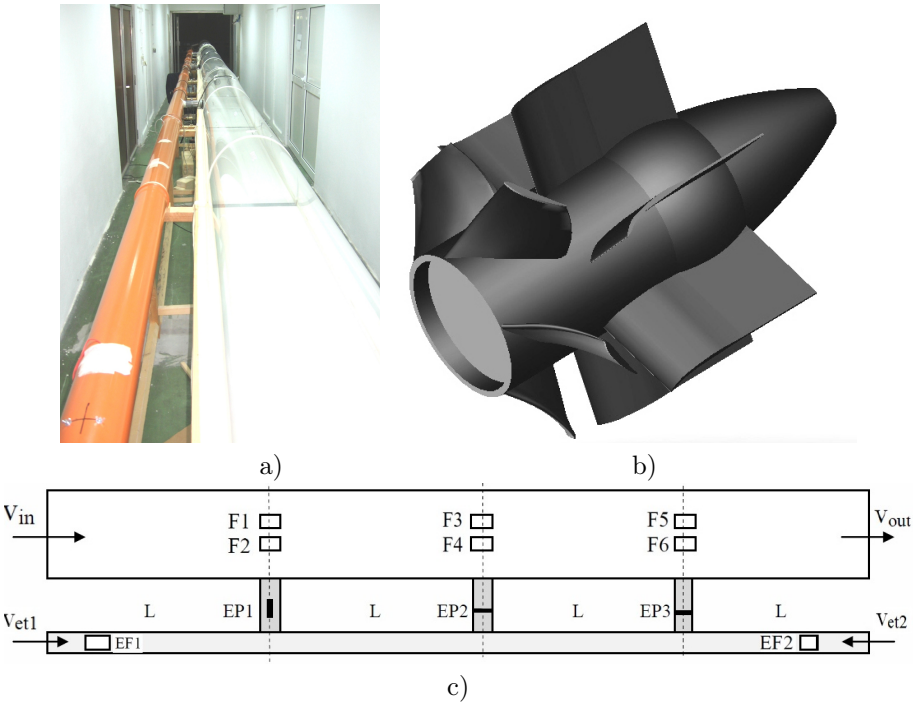

FIGURE 1. (a) Installation photo, (b) 3D CAD model of the fan (shroud is removed), (c) Scheme of the instalation.

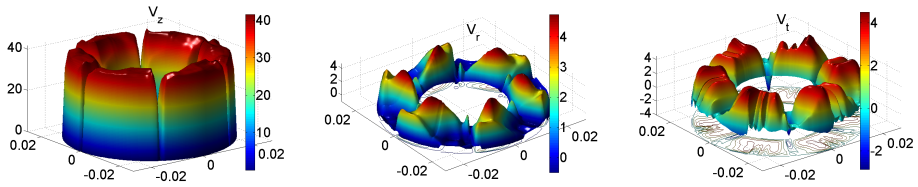

FIGURE 2. Time-averaged velocity components of fan exit turbulent field: (a) Axial v_z, (b) Radial v_r, (c) Tangential v_z.

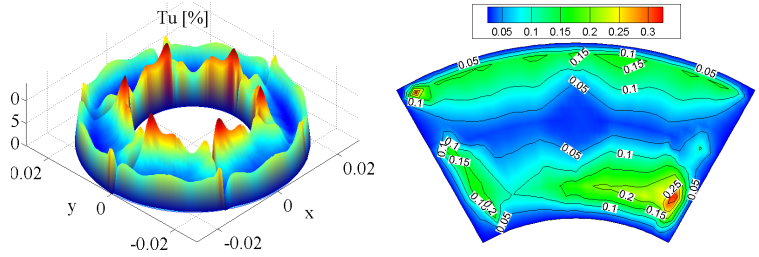

FIGURE 3. Fan flow turbulence properties: a) intensity $Tu\%$ over the whole fan exit cross section area, b) dimensionless TKE (1/6 of flow's exit plane is shown).

(0.564) and the hydraulic resistance coefficients of the used vehicle models: see Table 2, and **[3]**. Results are given for the empty tunnel flow in Table 1, and with stationary vehicle models in Table 3.

TABLE 1. Measured and derived values for flow in traffic-free model tunnel.

$T[N]$	$v[m/s]$	$w[m/s]$	$1-v/w[/]$	$\eta_i[/]$
≈ 7.2	4.175	25	0.83	≈ 0.70
≈ 13	6.27	33.5	0.81	≈ 0.85

Two traffic-load densities where adopted corresponding to two load regimes: normal (corresponding to a real tunnel with 80 km/h vehicle speed) and congested (at 10 km/h), **[3]**. The number of vehicles is estimated using RVS formulae **[3]**. For the scaled conditions of model tunnel and traffic share of 25 % of large vehicles (buses) and 75 % passenger cars, the proper number of vehicles is: a) ~ 43 passenger vehicles and 11 buses in the congested-traffic case; b) $\sim$ 11 passenger vehicles and 3 busses, at the 80 km/h regime case. To determine the hydraulic resistance coefficients of the used model-vehicles an experiment was conducted. The obtained values are reported in Table 2.

TABLE 2. Measured values of hidraulic resistances: streamlined and opposite orientations.

Vehicle	ζ_+	ζ_-
Car	≈ 0.49	≈ 0.71
Bus	≈ 1.1	≈ 1.1

From the conducted experiments, the following values of k_1 and η_i are determined, see Table 3:

TABLE 3. Measured and derived values for traffic loaded tunnel flow.

Reg.	$T\,[N]$	$v\,[m/s]$	$w\,[m/s]$	k_1	η_i
a)	≈ 12.8	≈ 4.12	33.5	0.88	≈ 0.80
b)	≈ 12.8	≈ 4.90	33.5	0.86	≈ 0.70

The η_i value is in the 0.70–0.85 range for fan-jet speeds above 30 m/s, in the empty tunnel flow case. In the traffic-loaded tunnel the results are in the range 0.70–0.80. To analyse the aforementioned issue and the relative influence of fan velocity field on the derived results, the numerical simulations are used further.

3. Numerical results

3.1. The mathematical model and the numerical grid. A CAD model of the tunnel installation was made to be identical to the real laboratory tunnel model. The fans were modeled accordingly, without particular approximations in their geometry, with an air-domain of the fan in the form of annuli between the fan's shroud and fan's hub. The experimentally determined properties of flow field were imposed there as boundary conditions. A hybrid-type of grid with 8.7 million elements in the fluid-domain was used. The elements consisted of prismatic and tetrahedral finite-volumes with boundary layers around fan surfaces, tunnel walls, vehicles-models were covered with layers of prismatic cells, in the form of prisms with triangular basis. The bulk mesh tetrahedral cell size spans from $\approx$ 1 mm (which is $\approx 50\,\%$ of the mean-value of integral length scales of the turbulent flow at the fan's exit) up to 25 mm (6 % of tunnel's hydraulic diameter) far from the fans. The wall-normal size of prismatic cells at the walls was fine enough to provide an average $y^+ \approx 1$. Flow was computed by numerically solving a system of incompressible RANS (Reynolds-averaged Navier–Stokes) equations in the Fluent flow solver [**3**]:

$$\frac{\partial \bar{v}_i}{\partial x_j} + \frac{\partial(\rho \bar{v}_i \bar{v}_j)}{\partial x_j} = -\frac{\partial \bar{p}}{\partial x_j} + \mu \frac{\partial^2 \bar{v}_j}{\partial x_j^2} + \frac{\partial R_{ij}}{\partial x_j} + f_i \tag{3.1}$$

$$\frac{\partial \rho}{\partial t} + \frac{\partial(\rho \bar{v}_i)}{\partial x_i} = 0 \tag{3.2}$$

where the $R_{ij} = -\rho\overline{v_i' v_j'}$ is the Reynolds turbulence stress tensor which has to be modeled. Turbulence was modeled using standard $k-\varepsilon$ and the $k-\omega$ SST turbulence models. Enhanced wall function approach was used with the $k-\varepsilon$ model. All the model constants had their default values ($C_\mu = 0.09$, $C_{1\varepsilon} = 1.44$, $C_{2\varepsilon} = 1.92$, $Pr_k = 1$, for $k-\varepsilon$; and for the $k-\omega$ SST model the constats were: $\alpha^*_\infty = 1$, $\alpha_\infty = 0.52$, $\beta^*_\infty = 0.09$, $\zeta^* = 1.5$). Appropriate boundary conditions were used and are discussed bellow. The iterative procedure was carried until all the residuals were reduced under 10^{-5}, and integral quantities showed no further change.

3.2. CFD cases and boundary conditions. Boundary conditions for presented CFD cases are listed in Table 4. Two layouts of the tunnel installation were considered: 1) A tunnel with no vehicles with the ventilation system exerting the thrust (cases S1, S2, S3, S4); 2) Tunnel with a congested traffic case occurring at a 10 km/h vehicle speeds in a two-lane traffic tunnel with a bi-directional traffic, in the two-opposite traffic lanes. The adopted vehicle share (in CFD-cases S5, S6, S7, S8) is approx. 30 % of large vehicles (model buses) vs model passenger cars. The number of vehicles in the analysed CFD tunnel was 38 passenger cars and 12 buses. A segment of $1.75D_{h1}$ near the exit tunnel-portal was clear from vehicles, while the first vehicles are $0.6D_{h1}$ downstream of the entry-portal.

TABLE 4. Overview of numerical cases and boundary conditions on the fans (and tunnel inlet).

Case	Model	Boundary conditions on fans
S1	$k-\varepsilon$	v_x, v_y, v_z
S2	$k-\omega$ SST	v_x, v_y, v_z,TKE
S3	$k-\omega$ SST	$v_z = \overline{w} = const, \bar{v}_x = 0, \bar{v}_y = 0$
S4	$k-\omega$ SST	$v_r \equiv 0 \rightarrow v^*_x, v^*_y, v_z$,TKE
S5	$k-\omega$ SST	with traffic, fans ON: v_x, v_y, v_z
S6	$k-\omega$ SST	with traffic, fans OFF: $(\triangle p_{\mathrm{tot}})_{in}$
S7	$k-\omega$ SST	with traffic, fans OFF: $v_{in} = v^{S5}_{tun}$
S8	$k-\omega$ SST	with traffic, fans ON, $Re = Re_{ob}$

For S1 case a full 3-component time-averaged turbulent flow field was prescribed on all fans, whereas in S2 an added Dirichlet condition of the measured TKE field at the fan exit was used. In S3 case a simplified fan representation as a constant axial-velocity flow jet was used. In S4 case the fields of v_x, v_y, v_z,TKE where used, but secondary flow was modified to represent an idealised nozzle with a zero radial component. Since the vehicle's surface have a velocity of 10 km/h = 2.78 m/s the obtained results represent an averaged (quasi-steady) picture, i.e., an averaged time-snapshot of a flow field, since the overall and averaged velocity results will be independent of the vehicle instantaneous position in this case.

To account for the hydraulic resistances induced by vehicles in the tunnel and isolate the ventilation system's efficiency in such specific flow conditions, two separate additional CFD cases were computed: S6 and S7. There the identical layout

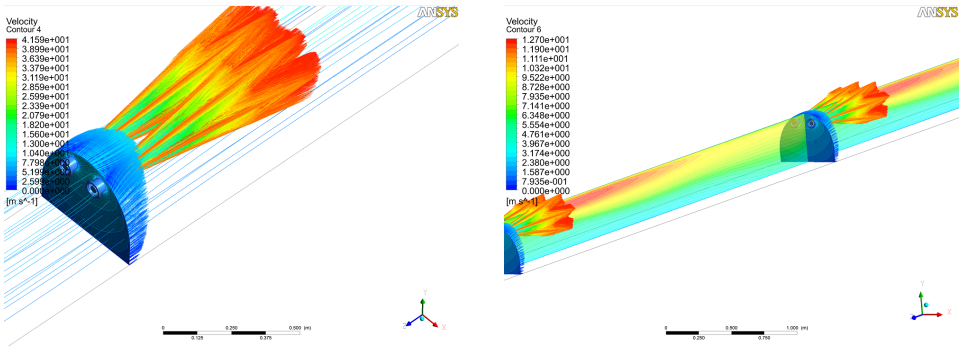

a) b)

FIGURE 4. Features of the computed flow fields: S1-case.

was used but the flow was induced not by operating the ventilation fans inside the analysed tunnel segment but by an external thrust source, outside of the considered CFD model-tunnel space. In S6 case a specified gauge total pressure δp_{tot} was prescribed, and in S7 case an inflow-velocity v_t at the tunnel entry portal. The air was able to freely pass through the fan annulus space. The air physical properties for all computed cases were: $\mu = 1.8 \cdot 10 \times 10^{-5}\,\text{Pa} \cdot s$, $\rho = 1.238\,\text{kg/m}^3$, and they correspond to the conditions of conducted laboratory experiments.

3.3. Numerical results for the empty tunnel flows. An overview of the computed velocity field is given in Figure 5. The velocity profile with respect to height above road-surface is presented in Figure 6. The axial time-averaged

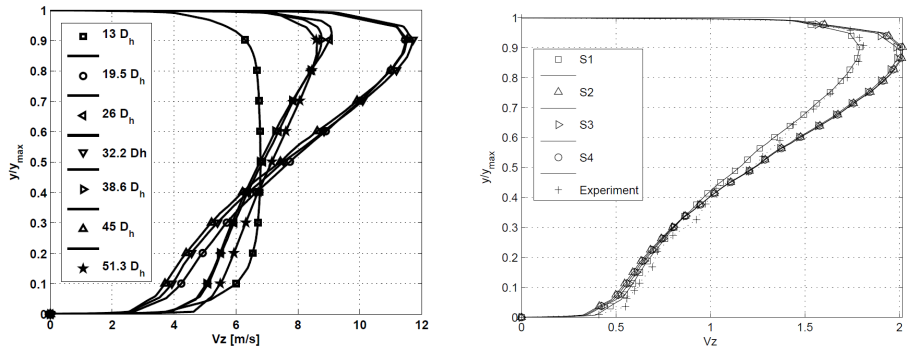

a) b)

FIGURE 5. Axial velocity with respect to height above road surface: a) in S1 case taken at different cross-sections along the tunnel: $13D_h$–$51.3D_h$ from the entry portal, b) Dimensionless axial velocity for S1–S4 cases, and the experiment, taken at the midpoint of the last tunnel section (L-long).

velocity profiles with respect to $y/y_{\max} = (0-1)$ were plotted for 7 different equidistant cross-sections downstream along the tunnel (at the exit planes of the fan batteries, the outlet portal and at the mid-sections between these): $v^* = \bar{v}_z/v_t$ The average value of y^+ over the tunnel wall with the used numerical grid was fairly low: 1.075. The axial velocity profile starts from a flat turbulent profile at the tunnel entry region, deforms along the tunnel into an asymmetrical profile with 2–3 times higher velocities near the tunnel ceiling. This occurs intermittently - from the F1F2 battery exit cross-section, it deforms from flat to asymmetric and later flattens again as the flow approaches the next fan battery. Some results are given in Table 5, including a skewness-coefficient of the axial velocity profile taken at the midpoint of the last section (L-long) of the tunnel; the point C is the midpoint of tunnel height at the symmetry-plane of the tunnel. Experimental result was obtained by a small Pitot tube, on the Lab. tunnel-model in the same ventilation operating conditions. The computed under-pressure value in the cross-section of the first fan battery F1F2 exit corresponds to the measured under-pressure in the Lab. model tunnel. It arises from the sum of all losses (entry loss, friction losses and the achieved fluid dynamic pressure).

TABLE 5. Comparison of results of S1–S4 cases and the experiment.

Case	v_t	v_C	k_1	η_i	Skewness coeff.
Exp	6.41	7.06	0.81	0.82	0.263
S1	6.44	7.19	0.813	0.825	0.204
S2	6.23	7.50	0.82	0.81	0.048
S3	6.64	7.60	0.807	0.891	0.072
S4	6.38	7.30	0.815	0.806	0.057

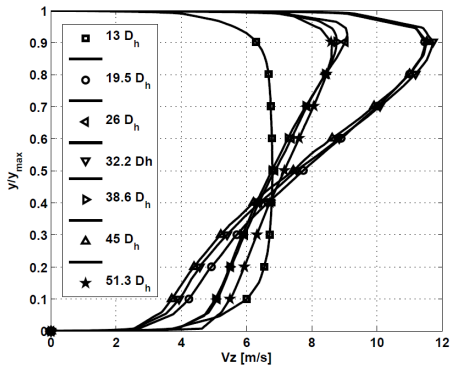

FIGURE 6. Average static pressure over a tunnel's cross-section along the tunnel at z/D_h downstream of the tunnel inlet (z is the distance from inlet). The values are taken at the each battery exit positions, and at midpoints between them.

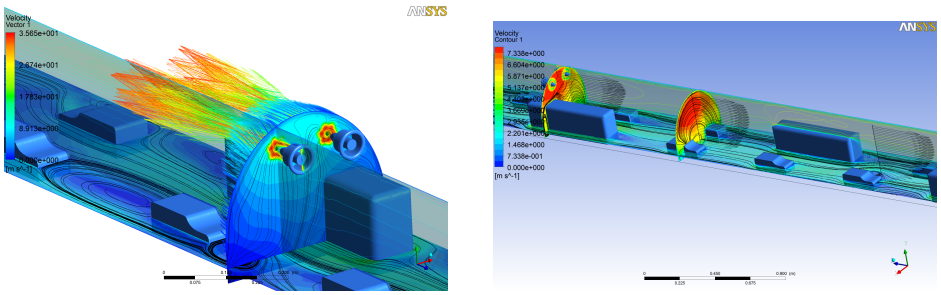

FIGURE 7. Velocity field in a traffic loaded funnel flow of S5 case (contours of absolute velocity).

3.4. Numerical results for flow in the tunnel with traffic. Flow features in the computed case S5, are given in Figure 8. In the presence of vehicles, the ventilation system exerted thrust is consumed to counteract the hydraulic resistances of the tunnel and the moving vehicles in the two traffic lanes with opposing traffic directions.

In order to evaluate the η_i, the required cumulative pressure drop could be, in principle, calculated using equation (1.2), but this requires an accurate information of specific vehicle's resistance coefficients, in the tunnel flow layout. To avoid this problem, two additional CFD cases are computed in identical geometrical layout as the previous S5-case, but the ventilation fans are switched "off" while the thrust is exerted by some source outside of the tunnel (upstream of the tunnel entry). Such CFD-case can reveal the velocity distribution which will occur in the tunnel much further downstream of the last operating fan-battery. Or, if the thrust is exerted by outside atmospheric sources (like wind or existing pressure differences between portals).

Thus, the boundary condition at the tunnel entry portal in S6 and S7 were:

a) In the S6-case a user-prescribed gauge total pressure of 90 Pa (which will produce tunnel velocity of similar value as in S5-case with working ventilation) and a supplied entry-loss coefficient;

b) In the S7-case the user-supplied constant-profile inlet velocity v_t, with a value prescribed as identical to the mean-value of flow velocity v_t computed in the S5-case where the same layout was studied but with the fans operating. In this way, it was possible to numerically compute the required pressure drop (and thus the effective thrust force T_{ef}) in the tunnel and using equation (1.1) rather than equation (1.2), isolate the η_i value in the S5 case, for such flow conditions with higher adopted traffic load (at 10 km/h layout).

The obtained results are given in Table 6.

It is reasonable to expect that for any given tunnel of sufficient length, the axial-velocity profile for an arbitrary cross-section along the tunnel should have the shape between these two estimated extremes, shown in Figure 8.

The S8 case was computed as equal to the S5-case, only the Reynolds number of flow was adjusted to correspond to a 20 times larger size tunnel, to evaluate

TABLE 6. Results for traffic-loaded tunnel flow cases

Case	User input b.c.	v_t	k_1	η_i
S5	$(v_x, v_y, v_z, k), \zeta_{in}$	4.77	0.863	≈0.86
S6	$\triangle p_{\text{tot}}$ at inlet, ζ_{in}	4.975	0.857	-
S7	v_{tun} at inlet	4.77	0.863	-
S8	$(v_x, v_y, v_z, k), \zeta_{in}$	4.95	0.858	≈0.92

a possible influence of Re number on the results in larger-scale object flow. The computed mean-value of axial velocity is approx. 3.9 % higher than in the S5-case with model-tunnel Re-number flow. It can be concluded that the Re number has a small influence on the results, and the obtained large-scale tunnel flow values of mean-flow velocity and ventilation efficiency are a few percent higher than for model-scale cases, whereas the average axial-velocity profile has a fairly similar shape, Figure 8.

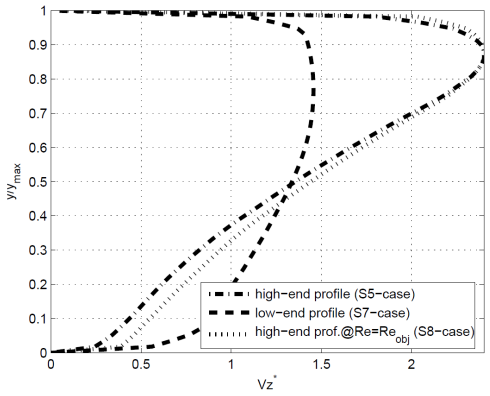

FIGURE 8. The envelope of possible dimensionless axial-velocity distribution in a traffic-loaded tunnel flow case, with respect to dimensionless height above road surface. Obtained by averaging the velocity profiles in the last segment, of characteristic length L (100 fan diameters).

The available static thrust of the ventilation system in the model-tunnel S1-S7 cases is approx. 13.6 N or 91.4 Pa. Given the same hydraulic resistance conditions in the tunnel in the three considered traffic-jam cases (S5–S7) it can be calculated that the efficiency of momentum transfer for the S5 case (with working ventilation) is 0.86, see Table 6.

An additional effect is observed by comparing the required thrust to a value which could be computed by using the experimentally determined resistance coefficients for these model-vehicles and equation (1.2), as is usually done in ventilation design. Using computed CFD results, it can be concluded that the appropriate effective values of hydraulic resistance coefficients of the here used model-vehicles

in the traffic layout analysed in traffic-cases S5, S6, S7 are lower than the values in Table 3, i.e., 0.30 vs 0.49 for passenger cars. Although values in Table 3 are subject to experimental error (which was an additional motivation to follow the approach presented in this chapter when computing traffic-loaded tunnel flow cases S5–S7) the appearance of lower effective values of vehicle-resistance coefficients in tunnel flows can be attributed to the drafting or slipstreaming phenomenon, given the congested traffic layout at vehicle speed 10 km/h.

4. Conclusions

The following results are obtained through the conducted experimental and numerical work:

• From the obtained results of flow measurements (on fans and on the scaled Lab. tunnel model) a value of efficiency for momentum transfer η_i for the tunnel with no traffic load is: $\approx$ 0.70–0.80, with higher values corresponding to higher fan-jet exit velocities (usually up to 35 m/s). For the flow in a Lab. model tunnel occupied with stationary vehicles the estimated η_i value is approx. 0.70.

• The analysis of the relative influence of the boundary conditions for a numerical simulation of tunnel flow and their effect on the achieved results, show that the fan's flow properties do have a non-negligible effect on the computed tunnel flow-field, in terms of the derived conclusions, like η_i values. The determined η_i value is approx. 0.80 with the used fans. The negative effect of the secondary flow components is assessed. Thus depending on the adopted boundary conditions in the numerical CFD case setup the η_i value varies from 0.81 to 0.89, i.e., by about 9 %;

• In a road-tunnel of a bi-directional traffic type, congested with vehicle-traffic in two traffic lanes occurring at the adopted standard critical regime of 10 km/h, the η_i value was assessed using CFD: the results show there isn't any noticeable deterioration of the ventilation efficiency η_i value in this specific case, compared to the traffic-free tunnel flow case. The η_i value of 0.86 is obtained, vs 0.85 value in the empty tunnel flows. The experiment showed lower values but its result here should be taken with caution given the difficulties in estimating the effective vehicle's resistance forces in the model-tunnel, and the mean-value of axial velocity in such disturbed flow;

• The effect of adopted boundary conditions on mean-value of flow velocity in S1–S4 cases is small (approx. 3.3 %), but more important on velocity profile asymmetry and the secondary flows in the tunnel. The maxima of axial velocity profile values under the tunnel ceiling, in the empty-tunnel flow cases, fall approx. within a 16 % range scatter;

• The real-scale Re-number numerical results (S8-case) are very similar to model-tunnel numerical results (S5-case), but with a computed value of the mean-flow velocity 4 % higher (using the same boundary conditions);

• In addition, the CFD results of tunnel flow with vehicle-traffic load reveal a possible slipstreaming effect of vehicle resistance in the traffic-jam case, i.e., possibly lower effective values of hydraulic resistance coefficients of the model-vehicles in the tunnel, compared to the values estimated experimentally for the same vehicle models in a single-vehicle tunnel flow;

• The asymmetrical shape of the axial velocity profile in the traffic-loaded tunnel-flow (at 10 km/h traffic density regime) is estimated in the form of an envelope of 2 limiting extremes. The shape of the velocity distribution will thus depend only on the distance of the analyzed cross-section with respect to the upstream-nearest operating fans, or if the fans do not operate but the flow is induced by atmospheric overpressure at the inlet, on the distance to the tunnel inlet. For any such tunnel flow situation, the distribution of velocity will have a shape within this envelope. Thus this result can be used as an appropriate inlet boundary condition, and/or initial condition in setting up a numerical simulation of flow and fire scenario, in a bi-directional traffic tunnel situation, with critical traffic load.

Acknowledgments. This work was funded by the grant from the Ministry of Education, Science and Technological Development (MESTD), Republic of Serbia, Project No. TR 35046 and Bilateral cooperation between MESTD, Serbia and Ministry of Science, Montenegro (2016–2018), coordinated between University of Belgrade, Faculty of Mechanical Engineering and University of Montenegro, Faculty of Mechanical Engineering: Investigation of the influence of turbulent swirl flow on the energy parameters of the axial fans by use of the contemporary measurement techniques, what is gratefully acknowledged.

References

1. F. Tarada, R. Brandt, *Impulse ventilation for tunnels - a state of the art review*, 13$^{\text{th}}$ International Symposium on Aerodynamics and Ventilation of Vehicle Tunnels, New Brunswick, New Jersey, 2009.
2. F. Tarada, *Design, testing and application of an energy-efficient longitudinal ventilation system*, 14$^{\text{th}}$ International Symposium on Aerodynamics and Ventilation of Tunnels, Dundee, Scotland, 2002.
3. M. Šekularac, *Analiza strujnih polja slozenih sistema ventilacije saobracajnih tunela*, PhD thesis,University of Montenegro, Faculty of Mechanical Engineering, 2015.
4. E. Jacques, P. Wauters, *Improving the Ventilation Efficiency of Jet Fans in Longitudinally Ventilated Rectangular Ducts*, Universite catholique de Lovain-la-Neuve, 2009.
5. A. D. Marteggani, G. Pavesi, C. Barbetta, *Uno studio sperimentale sulla ventilazione longitudinale nelle gallerie*, Gallerie e grandi opere sotterranee **48** (1996).
6. P. Levoni, D. Angeli, E. Stalio, E. Agnani, G. S. Barozzi, M. Cipollone, *Fluid-dynamic characterisation of the Mont Blanc tunnel by multi-point airflow measurements*, Tunneling and Underground Space Technology **48** (2015), 110–122.
7. E. Eftekharian, D. Alireza, O. Abouali, J. Meigolinedjad, G. Ahmadi, *A numerical investigation into the performance of two types of jet fans in ventilation of an urban tunnel under traffic jam conditions*, Tunneling and Underground Space Technology **44** (2014), 56–67.
8. Y. Wu, M. Z. A. Bakar, *Control of smoke flow in tunnel fires using longitudinal ventilation systems - a study of the critical velocity*, Fire Safety Journal **35** (2000), 363–390.
9. H. Ingason, Y. Z. Li, *Model scale fire tests with longitudinal ventilation*, Fire Safety Journal **45** (2010), 371–384.
10. L. Barbato, F. Cascetta, M. Musto, G. Rotondo, *Study of critical velocity and backlayering length in longiudinally ventilated tunnel fires*, Fire Safety Journal **45** (2010), 361–370.
11.] J. S. Roh, S. S. Yang, H. S. Ryou, M. O. Yoon, Y. T. Jeong, *An experimental study on the efect of ventilation velocity on burning rate in tunnel fires - heptane pool fire case*, Building and Environment **45** (2008), 1225–1231.
12. F. Tarada, *New prospectives on the critical velocity for smoke Control*, International Symposium on Tunnel Safety and Security **3**, 2009.

13. V. Betta, F. Cascetta, M. Musto, G. Rotondo, *Fluid dinamic performance of traditional and alternative jet fans in tunnel longitudinal ventilation systems*, Tunneling and Underground Space Technology, **25** (2010), 415–422.
14. L. Barbato, F. Cascetta, M. Musto, G. Rotondo, *Fire safety investigation for road tunnel ventilation systems - a overview*, Tunneling and Underground Space Technology, **43** (2014), 253–265.
15. M. K. Camby, E. W. M Lee, A. C. K. Lai, *Impact of location of jet fan on airflow structure in tunnel Fire*, Tunneling and Undeground Space Technology **27** (2012), 30–40.
16. M. Šekularac, *Experimental determination of tunnel ventilation ducted fan performance*, Thermal Science **53**(4) (2014), 1237–1242.
17. P. Vukoslavčeević, J. Wallace, *A 12-sensor hot-wire probe to measure the velocity and vorticity vectors in turbulent flow*, Springer Ser. Meas. Sci. Technol. **7**(7) (1996), 1451–1461.
18. Ansys, *Ansys, Fluent solver theory guide*, ANSYS, 2013.

ЕКСПЕРИМЕНТАЛНА И НУМЕРИЧКА АНАЛИЗА СТРУЈНОГ ПОЉА И ПЕРФОРМАНСИ ВЕНТИЛАЦИЈЕ У САОБРАЋАЈНОМ ТУНЕЛУ ВЕНТИЛИСАНОМ ПУТЕМ АКСИЈАЛНИХ ВЕНТИЛАТОРА

Резиме. Ради испитивања струјања ваздуха у вентилисаним саобраћајним тунелима, умањени модел типског друмског саобраћајног тунела са одговарајућим системо вентилације на бази аксијалних вентилатора, је конструисан и направљен у лабораторији. Циљ овог рада је струјно поље у тунелу двосмјерног саобраћаја, са двије коловозне траке. Са размјером од око 1:20, а дужином 20.52 m модел представља око 400 m дуг стварни тунел објекат. Модел се састоји од двије паралелне тунелске цијеви, гдје је главни тунел (хидрауличког пречника $\approx$ 400 m има облик попречног пресјека умањеног друмског тунела објекта. Други тунел ($D_{h2} \approx 0.16$ m) је мањих димензија и кружног је попречног пресјека, а користи се само као модел евакуационог тунела симулирајући струјање ваздуха из главног саобраћајног у евакуациони тунел. Дакле два тунела су повезани евакуационим путевима, опремљеним подесивим преградним вратима. Комбиновањем експементалног и рада на рачунару, струјно поље и перформансе вентилационог система су истражене. Поље брзине и турбуленције на излазу из вентилатора вентилационог система је дефинисано експериментално користећи термалну анемометрију. Ови подаци су даље обрађени да би се употријебили при нумеричком симулирању струјног поља у тунелу путем CFD. Ефикасност преноса импулса (η_i, Кемпф фактор) подужне вентилације је одређена, те ефекат који задати гранични услови и ниво њихове детаљности имају, у оквиру CFD симулације струјног поља у тунелу, са аспекта тачности резултата, поља брзине и срачунатог η_i. На крају, случај "загушеног" тунела (саобраћајем) је проучен путем експерфимента и CFD. Тешкоће у дефинисању потребне силе потиска вентилације у ситуацији оптерећеног саобраћаја су дискутоване, и срачуната је ефикасност преноса импулсе вентилације. На бази ових резултата, два крајња случаја облика распоређеле аксијалне компоненте брзине ваздуха у тунелу у функцији висине од површине друма, у овој врсти тунела и саобраћаја, је дефинисана путем CFD. Последњи резултат се може користити као реалистичан гранични услов (као улазни гранични услов и/или почетни услов) за нумеричке анализе струјног поља и преноса топлоте у сличним тунелима у условима саобраћајног загушења, што је критична ситуација за пројектовање.

Laboratory for Fluid Mechanics and Energy Processes
Faculty of Mechanical Engineering
University of Montenegro
Podgorica, Montenegro
milans@ac.me

Hydraulic Machinery and Energy Systems Department
Faculty of Mechanical Engineering
Univrsity of Belgrade
Belgrade, Serbia
nolebb@gmail.com

(Received 01.12.2017)
(Available online 05.09.2018)